

The approximate local radiation condition (8.61) is implemented in essentially the same manner as the nonlocal condition (8.55), except that instead of Fourier transforming w , applying (8.55), and then inverse transforming to obtain the boundary values for the pressure, (8.61) is solved to compute the grid-point values of P directly from the grid-point values of w . A tridiagonal system for the grid-point values of P along the top boundary is obtained when the second derivatives in (8.61) are approximated by a standard three-point finite difference. Special conditions are required at those points adjacent to the lateral boundaries, where it can be advantageous to use the less accurate approximation

$$\left(b_1 - b_2 \frac{\partial^2}{\partial x^2}\right) P = Nw.$$

This relation, which is derived from (8.55) using the approximation $|k| \approx b_1 + b_2 k^2$, does not require any assumption about the horizontal variation of w at the lateral boundaries. Some assumption is nevertheless required about the variation of P near the boundary, and satisfactory results have been obtained by setting $\partial P / \partial x$ to zero in the upper corners of the domain.

8.4 Wave-Absorbing Layers

One way to prevent outward-propagating disturbances from reflecting back into the domain when they encounter the boundary is to place a wave-absorbing layer at the edge of the domain. Wave-absorbing layers are conceptually simple and are particularly attractive in applications for which appropriate radiation boundary conditions have not been determined. Wave-absorbing layers also allow "large-scale" time tendencies to be easily imposed at the lateral boundaries of the domain. These large-scale tendencies might be generated by a previous or concurrent coarse-resolution simulation on a larger spatial domain. The chief disadvantage of the absorbing-layer approach is that the absorber often needs to be rather thick in order to be effective, and significant computational effort may be required to compute the solution on the mesh points within a thick absorbing layer. Considerable engineering may also be required to ensure that a wave-absorbing layer performs adequately in a given application.

Suppose that a radiation upper boundary condition for the two-dimensional linearized Boussinesq equations (8.37)–(8.40) is to be approximated using a wave-absorbing layer of thickness D . This absorbing layer can be created by defining a vertically varying viscosity $\alpha(z)$ and adding viscous terms of the form $\alpha(z)\partial^2 u / \partial x^2$, $\alpha(z)\partial^2 w / \partial x^2$, and $\alpha(z)\partial^2 b / \partial x^2$ to the right sides of (8.37), (8.38), and (8.39), respectively. The viscosity is zero in the region $z \leq H$ within which the solution is to be accurately approximated and increases gradually with height throughout the layer $H < z \leq H + D$. A simple rigid-lid condition, $w = 0$, can be imposed at the top of the absorbing layer. The performance of this ab-

sorbing layer is largely determined by the vertical profile of the artificial viscosity $\alpha(z)$ and the total absorbing-layer depth D . The total viscosity in the absorbing layer must be sufficient to dissipate a wave before it has time to propagate upward through the absorbing layer, reflect off the rigid upper boundary, and travel back down through the depth of the layer. It might, therefore, appear advantageous simply to set α to the maximum value permitted by the stability constraints of the finite-difference scheme. Reflections will also occur, however, when a wave encounters a rapid change in the propagation characteristics of its medium, and as a consequence, reflection will be produced if the artificial viscosity increases too rapidly with height. The only way to make the total damping within the wave absorber large while keeping the gradient of $\alpha(z)$ small is to use a relatively thick wave-absorbing layer.

The reflectivity of a wave-absorbing layer also depends on the characteristics of the incident wave. Klemp and Lilly (1978) examined the reflections produced by a wave-absorbing layer at the upper boundary in a problem where hydrostatic vertically propagating gravity waves were generated by continuously stratified flow over topography. They found that although a very thin absorbing layer could be tuned to efficiently remove a single horizontal wave number, considerably deeper layers were required to uniformly minimize the reflection over a broad range of wave numbers. In order to ensure that the absorbing layer was sufficiently deep, and to guarantee that the numerical solution was adequately resolved within the wave-absorbing layer, Klemp and Lilly devoted the entire upper half of their computational domain to the absorber. The efficiency of their numerical model could have been increased by a factor of two if the wave-absorbing layer had been replaced with the radiation upper boundary condition described in the preceding section.

The finding that effective wave-absorbing layers must often be rather thick is also supported by Israeli and Orszag (1981), who examined both viscous and Rayleigh-damping absorbing layers for the linearized shallow-water system of the form

$$\frac{\partial u}{\partial t} + \frac{\partial \eta}{\partial x} = \nu(x) \frac{\partial^2 u}{\partial x^2} - R(x)u, \quad (8.65)$$

$$\frac{\partial \eta}{\partial t} + c^2 \frac{\partial u}{\partial x} = 0 \quad (8.66)$$

on the domain $-L \leq x \leq L$. Boundary conditions were specified for $u(-L, t)$ and $u(L, t)$; no boundary conditions were specified for η . Since there is one inward-directed characteristic at each boundary, the specification of u at each boundary yields a well-posed problem for all nonnegative ν . Numerical solutions to the preceding system can be conveniently obtained without requiring numerical boundary conditions for η by using a staggered mesh where the outermost u points are located on the boundaries and the outermost η points are $\Delta x/2$ inside those boundaries (see Section 3.1.2). Israeli and Orszag demonstrated that better results could be obtained using Rayleigh damping ($R > 0$, $\nu = 0$) than by using vis-

the artificial viscosity in the absorbing layer to propagate upward, and travel back appear advantageous. However, when a wave is of its medium, and artificial viscosity increases damping within the wave use a relatively thick

the characteristics of reflections produced by where hydrostatic vertically stratified flow absorbing layer could be, considerably deeper over a broad range of was sufficiently deep, y resolved within the per half of their commercial model could ing layer had been rebed in the preceding

ten be rather thick is ed both viscous and low-water system of

(8.65)

(8.66)

pecified for $u(-L, t)$. Since there is one fication of u at each Numerical solutions t requiring numerical e outermost u points e $\Delta x/2$ inside those ted that better results)) than by using vis-

cous damping ($\nu > 0, R = 0$) because the erroneous backward reflection induced by the Rayleigh damping is less scale dependent than that generated by viscous damping. Israeli and Orszag also suggested that superior results could be obtained by using a wave-absorbing layer in combination with a one-way wave equation at the actual boundary. When using both techniques in combination, the one-way wave equation must be modified to account for the dissipation near the boundary. For example, an approximate one-way wave equation for the right-moving wave supported by (8.65) and (8.66) with $\nu = 0$ and R constant is

$$\frac{\partial u}{\partial t} + c \frac{\partial u}{\partial x} = -\frac{R}{2}u. \quad (8.67)$$

The problem considered by Israeli and Orszag is somewhat special in that it can be numerically integrated without specifying any boundary conditions for η . If a mean current were present, so that the unapproximated linear system is described by (8.2), then numerical boundary conditions would also be required for η in order to evaluate $U \partial \eta / \partial x$. The specification of η at the boundary where the mean wind is directed inward, together with specification of u at each boundary, will lead to an overdetermined problem. Nevertheless, Davies (1976, 1983) has suggested that wave-absorbing layers can have considerable practical utility even when they require overspecification of the boundary conditions.

As a simple example of overspecification, consider the one-dimensional scalar advection equation with $U > 0$. Davies's absorbing boundary condition for the outflow boundary corresponds to the mathematical problem of solving

$$\frac{\partial \psi}{\partial t} + U \frac{\partial \psi}{\partial x} = -R(x)(\psi - \psi_b) \quad (8.68)$$

on the domain $-L \leq x \leq L$ subject to the boundary conditions

$$\psi(-L, t) = s(t), \quad \psi(L, t) = \psi_b(t).$$

The Rayleigh damper is constructed such that $R(x)$ is zero except in a narrow region in the vicinity of $x = L$. The boundary condition at $x = -L$ is required to uniquely determine the solution, since the characteristic curves intersecting that boundary are directed into the domain. The boundary condition at $x = L$ is, however, redundant, since no characteristics are directed inward through that boundary, and as noted by Oliger and Sundström (1978), the imposition of a boundary condition at $x = L$ renders the problem ill-posed.

The practical ramifications of this ill-posedness are, however, somewhat subtle. One certainly cannot expect to obtain a numerical solution that converges to the unique solution to an ill-posed problem. This behavior is illustrated by the test problem shown in Fig. 8.7, in which (8.68) was approximated as

$$\frac{\phi_j^{n+1} - \phi_j^{n-1}}{2\Delta t} + U \frac{\phi_{j+1}^n - \phi_{j-1}^n}{2\Delta x} = R_j(\phi_j^{n+1} - \phi_N)$$

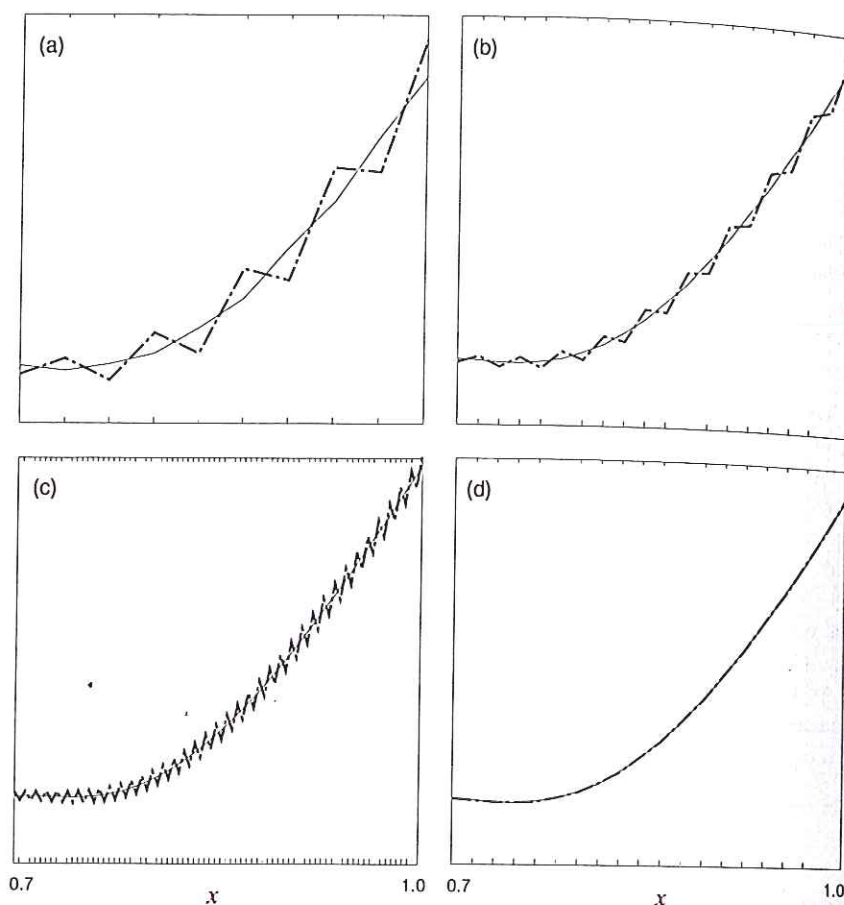


FIGURE 8.7. Comparison of numerical solutions to the advection equation obtained using a Rayleigh damping wave absorber (dot-dashed curve) or linear extrapolation (thin solid curve) and Δx equal to (a) $1/32$, (b) $1/64$, or (c) $1/256$. In (d) the magnitude of the Rayleigh damping coefficient is doubled and $\Delta x = 1/64$.

on the interval $-1 \leq x \leq 1.125$. Here N is the spatial index of the grid point on the right-boundary, and the Rayleigh damping coefficient is defined as

$$R(x) = \begin{cases} 0, & \text{if } x \leq 1; \\ \alpha(1 + \cos[8\pi(x - 1)]), & \text{otherwise,} \end{cases}$$

so that the region $1 \leq x \leq 1.125$ contains the wave absorber. The Courant number was one-half, U was 1, and ϕ was fixed at a constant value of zero at the right and left boundaries. The initial condition was

$$\psi(x, 0) = \begin{cases} 0, & \text{if } |x - \frac{1}{2}| \geq 1; \\ \cos^2[\pi(x - \frac{1}{2})], & \text{otherwise.} \end{cases}$$

A second solution to the linear extrapolation wave-absorbing layer.

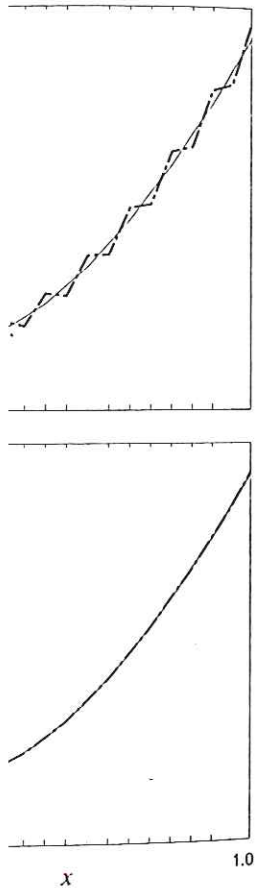
Figure 8.7 focuses on the region $0.7 \leq x \leq 1$. The initial pulse has peak amplitude 1. The absorbing layer at $x = 1$ is chosen such that the width of the absorbing layer, Δx , is fixed, Δt is also fixed. Both solution methods continue to extrapolate the boundary condition by a factor of four in Figure 8.7. The solution continues to extrapolate the boundary condition, but does not exhibit a significant error. Further increase in the wave-absorbing coefficient is, however, exhibited in the condition.

If α is doubled, the two preceding high-resolution solutions are very similar to the additional high-resolution underlying mathematics to the correct solution outside the absorbing applications. Of course, the recommended in situ solution can be formulated to make a clear-cut recommendation for open boundary conditions. A range of numerical approximations to the damping absorber can be used. Caution is, nevertheless,

A second solution, indicated by the thin solid line in Fig. 8.7, was obtained using the linear extrapolation boundary condition (8.18) at $x = L$ instead of using a wave-absorbing layer.

Figure 8.7 focuses on the trailing edge of the disturbance in the subdomain $0.7 \leq x \leq 1$. The time shown is $t = \frac{3}{4}$, at which time three-quarters of the initial pulse has passed into the wave-absorbing layer. The interface between the absorbing layer and the interior domain coincides with the right edge of each plot. The horizontal grid spacing for the simulation shown in Fig. 8.7a is $1/32$ and α is chosen such that $R_N \Delta t$ is unity. Considerable reflection is produced by the absorbing layer, which is only four grid points wide. Weaker reflection is also produced by the extrapolation boundary condition. Figure 8.7b shows the solutions to the same physical problem obtained after halving Δx , which increases the width of the absorbing layer to eight grid points. Since the Courant number is fixed, Δt is also halved, and the maximum value of $R_N \Delta t$ is reduced to one-half. Both solutions are improved by this increase in resolution, but the sponge layer continues to produce significantly more reflection than that generated by the extrapolation boundary condition. The grid spacing is reduced by an additional factor of four in Fig. 8.7c, so that $\Delta x = 1/256$. This increase in numerical resolution continues to improve the solution obtained with the extrapolation boundary condition, but does not improve the solution obtained with the wave-absorbing layer. Further increases in the resolution do not make the solution computed with the wave-absorbing layer converge toward the correct solution. Such convergence is, however, exhibited by the solution obtained using the extrapolation boundary condition.

If α is doubled, the wave-absorbing layer does perform much better in the two preceding higher-resolution simulations. Figure 8.7d shows a simulation with $\Delta x = 1/64$ and $R_N \Delta t = 1$ in which the performance of the wave-absorbing layer is very similar to that obtained using the extrapolation boundary condition. Additional high-resolution simulations suggest that although the ill-posedness of the underlying mathematical problem prevents the solution from uniformly converging to the correct solution within the absorbing layer as $\Delta x \rightarrow 0$ and $\Delta t \rightarrow 0$, the error *outside the absorbing layer* remains small and may be acceptable in some applications. Of course, the use of a Rayleigh-damping absorber is not actually recommended in situations, such as this, where an exact open boundary condition can be formulated for the original partial differential equation. It is harder to make a clear-cut recommendation in the vast majority of cases, for which exact open boundary conditions are not available. It is certainly possible that over some range of numerical parameters, the errors generated by the ill-posed Rayleigh damping absorber can be less than those obtained using well-posed numerical approximations to overly reflective boundary conditions. Indeed, the Rayleigh-damping absorber appears to have been used successfully in a variety of studies. Caution is, nevertheless, advised.



on equation obtained using
ar extrapolation (thin solid
magnitude of the Rayleigh

dex of the grid point on
is defined as

≤ 1 ;
erwise,

er. The Courant number
e of zero at the right and

≥ 1 ;
e.